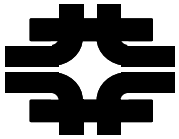

R.P. NOTE 139

Notes on Radiation Shielding for Two-Dimensional Extended Sources: Some Examples

Alex Elwyn

(October 2002)

Author: _____ Date: _____
A. Elwyn

Reviewed: _____ Date: _____
K. Vaziri

Reviewed: _____ Date: _____
N. Grossman

Approved: _____ Date: _____
D. Cossairt
Associate Head, Radiation Protection

Approved: _____ Date: _____
Bill Griffing
Head, ES&H Section

Distribution via Electronic Mail*

R. P. Note 139

Notes on Radiation Shielding for Two-Dimensional Extended Sources: Some Examples

Alex Elwyn

1. Introduction

This manuscript presents some simple results on the attenuation of gamma rays for extended radiation sources. The motivation for this study arises from concern about dose equivalent rates to personnel in connection with the residual radioactivity associated with the handling of material components irradiated at the NuMI experiment. An EXCEL spreadsheet and documentation for its use in connection with the handling of radioactive components had been previously prepared by Bennett (Be00). The present report is meant to be a summary of some of the formulae (and some examples) that were used in preparing that spreadsheet, but it does not represent instructions for using it.

There are many textbooks and monograms on the determination of dose from extended sources of radiation (see, e.g., Mo73, Ka78, Ch84, Sh96). There are also a number of compilations of the pertinent formulae. (See, e.g., Fo78). By far the most extensive and complete reference on the shielding of gamma radiation is the Engineering Compendium on Radiation Shielding, Vol. 1 (Ja68). Here, we present a few of the pertinent expressions and give examples of some simple calculations for various extended sources that may be appropriate for NuMI, or other experiments dealing with radioactive components. In this report, dose attenuation is defined as the dose at the distance *h* divided by the incident dose.

2. Attenuation From a Line Source: Unshielded and Shielded by a Slab

For a point on the perpendicular bisector of a line source of length *L* and a distance *h* away, and for a slab shield of material with thickness *t*:

$$Att'n = \frac{1}{2\pi h} F(\Theta, \mu t), \qquad (1)$$

where $F(\Theta, b) = \int_0^{\Theta} e^{-b \sec\Theta'} d\Theta' \approx \Theta e^{-b} \overline{F(\Theta, b)}$ is the Sievert Integral

and $\overline{F}$ is shown in Fig.1 (Ch84). μ is the linear attenuation coefficient for gamma rays in the shield material and depends on the photon energy, $b = \mu t$=number of mean free paths (mfp), and Θ is the angle whose tangent is *L/(2h)* and must be in units of radians. Some results from the application of this formula are shown below. Note that Eq. 1 does not take photon buildup due to the attenuating medium into account. See Sect. 3 for further discussion.

In Fig. 2, the attenuation of absorbed dose as a function of thickness for an Fe shield is displayed for both a point source and a 10 foot long line source (from Eq. 1) for 1 MeV gamma rays. The upper part displays the attenuation at a distance of 2.5 feet from the source, while the lower part gives the results at a distance of 10 feet. Both curves show an exponential dependence with about the same value of the exponent, 0.47 cm^{-1}, which is the linear attenuation coefficient μ for 1 MeV gamma rays in Fe. Thus, the dependence on shield thickness of the attenuation of a line source is the same as that of a point source, although the absolute attenuation is less by about two orders of magnitude. That is, the absorbed dose after any shield thickness is smaller for the point source.

Figs. 3 and 4 show the dependence of the attenuation on the distance *h* for four different shield thicknesses at three values of *h*. While the point source can be represented by an h^{-2} dependence for all values of shield thickness, the expected h^{-1} dependence for the line source is only observed for very thick shields. The upper part of Fig. 5 shows the dependence of the exponent in a power law fit to the *h*-dependence of the attenuation as a function of Fe shield thickness; it can be seen to approach h^{-1} for thick shields. The reason is based on the properties of the *F*-Function itself, and is illustrated in the lower plot in Fig.5 where it is observed that the exponent of the fits to the *F*-Function alone approaches 0 for thick shields so that the fit to the attenuation as a function of *h* approaches $(2\pi h)^{-1}$.

3. Photon Buildup

For any photon source and attenuating medium there are two components of total photon fluence that reach the detector. One is the unscattered component which consists of photons that reach the detector without interacting with the attenuating medium. The second is the component that consists of photons which have been scattered at least once in the medium, along with any secondary photons such as x-rays, etc., that may be produced. The buildup factor is defined as the ratio of the total dose to the unscattered dose. It is usually defined for point sources, but can be applied to distributed sources shielded by attenuating media.

There are a number of empirical approximations used in the calculation of buildup factors. One of the simplest is the Taylor approximation. It is usually written for two terms only as

$$B(E_0, \mu t) \approx A_1 e^{-\alpha_1 \mu t} + A_2 e^{-\alpha_2 \mu t}, \qquad (2)$$

where the coefficient $A_2 = 1 - A_1$, and A_1, α_1, α_2 are shown for Fe and concrete as a function of photon energy in Fig. 6 (Fo78). To use these coefficients for, e.g., the shielded line source discussed in Sect. 2, the attenuation coefficient μ is replaced by $(1+\alpha_1)\mu, (1+\alpha_2)\mu$, and the attenuation expression in Eq. 1 is therefore modified as follows:

$$Att'n = \frac{1}{2\pi h}[A_1 F(\Theta,(1+\alpha_1)\mu t) + (1-A_1)F(\Theta,(1+\alpha_2)\mu t)]. \qquad (3)$$

The buildup factor itself for 1-MeV photons, defined by Eq. 2, is shown as a function of the number of mfp (where one mfp=μ^{-1}) (upper plot) and thickness *t* (lower plot) in Fig. 7, for both concrete (μ=0.149 cm^{-1}) and Fe (μ = 0.47 cm^{-1}). In fact, the attenuation including buildup found by simply multiplying the attenuation without buildup by the factors shown in Fig. 7 gives results equal, within a few percent, to those calculated from Eq. 3 for Fe shields up to 2 feet thick.

4. Attenuation from Area Sources

For a point located on the axis of an isotropic disk source of radius *a* at a distance *h* away from the source, the attenuation can be written (see, e.g., Ch84) as

$$Att'n = (1/2)\ln(1+(a/h)^2)\,. \qquad (4)$$

This expression can be used to determine the direct (line-of-sight) component of attenuated absorbed dose at the exit of a cylindrical duct in shielding.

For an isotropic rectangular surface source of width *w* and length *l* at a point on the axis of symmetry perpendicular to the rectangle and a distance *h* away the attenuation is given (Ch84) by

$$Att'n = (2/\pi)\tan^{-1}[\frac{\varepsilon}{\eta}(1+\varepsilon^2+\eta^2)^{-0.5}], \qquad (5)$$

where $\varepsilon = \frac{w}{l}$ and $\eta = \frac{2h}{l}$. Evaluation of the line-of-sight component for a rectangular duct can be determined using this expression. It should be noted that the attenuation for both disk and rectangular surface sources is the same for sources of the same area. This is shown in the top plot of Fig. 8 for a distance *h*=6 feet (182.9 cm) or, equivalently, for a 6 foot long duct. The lower plot shows the attenuation as a function of the width (for a rectangular or square duct) or radius (for cylindrical duct).

5. Attenuation Through Cylindrical Ducts in Shielding

The contribution to the radiation that streams through ducts in shielding arises from three components. These are the direct (line-of-sight) component, a component from radiation that penetrates the duct walls at the entrance to the duct, and a component from radiation reflected from the duct walls. While a complete treatment requires Monte Carlo methods to track the radiation through the duct, Chilton et al (Ch84) and Shultis and Faw (Sh96) describes some analytic approximations for treating each of these parts. An example, based on simplified assumptions for the analytic formulae, follows. The discussion is

limited to straight ducts and the source strength for monoenergetic 1-MeV gamma rays is assumed to be uniform and isotropic across the duct entrance.

For a cylindrical duct with radius a = 0.5 foot (15.2 cm) and length h = 6 feet (183 cm), the attenuation due to line-of-sight for a detector placed at the center point of the exit face is just given by the expression for the disk source (Eq. 4) if the medium in the duct is non-attenuating (such as air), and is shown in Fig. 8.

The wall penetration component for a duct within an attenuating medium (an Fe shield, e.g.) with gamma ray attenuation coefficient μ, is discussed by Chilton et al (see Sect. 9.2.3 in ref. Ch84) as well as by Shultis and Faw (Sh96). For ducts in Fe shields (μ = 0.47 cm^{-1}) with a radius on the order of $a = 0.5$ foot (15.2 cm) and lengths of $h = 3$-10 feet (91-305 cm), μh = 43-143 mfp and $a/h = 0.17$-0.05. Under these conditions, as can be inferred from Fig.9 (or from Fig. 9.9 in Ch84 or Fig. 7.19 in Sh96), the wall penetration contribution is negligibly small. As observed, for μh in the range mentioned above (i.e., 43-143 mfp) the attenuation would be well below that shown in the Fig. and consequently much less important than the line-of-sight component.

For the wall-reflected component it is generally single scattering that constitutes the major part of the total contribution. A simplified treatment for single scattered reflection from the surface of a duct is given in Ch84 and Sh96. The albedo method, an approximate procedure for treating radiation reflection from surfaces, is generally used. For a detector placed at the center of the exit of a duct of a given aspect ratio (a/h), the attenuation defined (as always) as the ratio of the dose at the center of the exit to the incident dose, is shown in Fig. 10 for 1-MeV photons incident with isotropic fluence. As observed, the single-scattered wall-reflection attenuation is at most 10% of that from the line-of-sight component.

6. Summary

This report discusses the attenuation of dose for two applications of extended sources: Shielded line sources and cylindrical ducts in shielding. While this is far from an extensive compilation of dose attenuation results from extended sources, it does summarize a few cases that are clearly appropriate for application at NuMI and other beamlines. The pertinent simple formulae for line sources and for the line-of-sight component for cylindrical ducts are shown and discussed, and estimates of the other components that contribute to the attenuation through a duct are revealed to be much less important.

7. Acknowledgment

I thank Kamran Vaziri for many useful discussions. Thanks also to Nancy Grossman and Don Cossairt for constructive comments on the manuscript.

8. References

Be00: S. Bennett, "NuMI Hot Horn #1 Handling 4.0 Read Me", Fermi National Accelerator Lab, unpublished report (2000).

Ch84: A. B. Chilton, J. K. Shultis, and R. E. Faw, Principles of Radiation Shielding, Prentice-Hall, Inc., New Jersey (1984).

Fo78: Anthony Foderaro, The Photon Shielding Manual, Pennsylvania State University (1978).

Ja68: R. G. Jaeger, E. P. Blizard, A. B. Chilton, M. Grotenhuis, A. Honig, T. A. Jaeger, and H. H. Eisenlohr, Eds., Engineering Compendium on Radiation Shielding, Springer-Verlag, New York (1968).

Ka78: K. R. Kase and W. R. Nelson, Concepts of Radiation Dosimetry, Pergamon Press, New York (1978).

Mo73: K.Z. Morgan and J. E. Turner, Eds., Principles of Radiation Protection, R. E. Krieger Co., New York (1973).

Sh96: J. K. Shultis and R. E. Faw, Radiation Shielding, Prentice-Hall PTR, New Jersey (1996).

9. Figure Captions

1. The function $\overline{F(\Theta,b)}$ in the expression for the Sievert Integral plotted as a function of Θ for various values of b, the number of mfp in the shielding material. (See Eq. 1).

2. Attenuation of dose as a function of shield thickness *t* for an Fe shield for both a point and a 10 foot long line source. The upper plot is at a distance of 2.5 feet from the source, and the lower plot gives the results at a distance of 10 feet. No photon buildup is included. To include buildup multiply each point by the appropriate factor for each shield thickness from Fig. 7. The exponential dependence is reduced to 0.41 cm^{-1} from 0.47 cm^{-1} with no buildup, as seen in the Fig.

3. The dependence of attenuation (not including buildup) on distance *h* from the source for both a point and a 10 foot line source for a 0 cm thick Fe shield (unshielded), and 7.44 cm (2.92 inch) thick Fe shield. To include buildup multiply each point by the appropriate factor for the given shield thickness from Fig. 7. This will not change the dependence on h in the fits.

4. The dependence of attenuation (not including buildup) on distance from the source for both a point and a 10 foot line source for both 17.4 cm (6.85 inch) and 74.5 cm (2.4 foot) thick Fe shields. (See comments in Fig. 3 caption).

5. The dependence on Fe shield thickness *t* of the exponent in a power law fit to the attenuation as a function of distance from the source *h*, for three different distances as in Figs. 3 and 4 (top plot). The bottom plot shows the same dependence for both the attenuation (from top plot) and the Sievert Integral *F* itself.

6. The coefficients in the Taylor expression Eq. 2 for the buildup factor for both Fe and concrete shields as a function of the photon energy.

7. The buildup factor as a function of mfp (μt) (upper plot) for both concrete and Fe shields, and as a function of shield thickness *t* (lower plot).

8. The line-of-sight attenuation for both cylindrical and square ducts in shielding as a function of the area of the duct opening (top plot), and as a function of the width or radius (bottom plot).

9. The wall penetration and line-of-sight contributions to the attenuation for a straight cylindrical duct in shielding (for isotropic 1-MeV photons) plotted as a function of aspect ratio (radius/length=*a/h* of duct) for various shield thicknesses, in mfp. The contribution from shields thicker than 10 mfp is very much smaller than the line-of-sight contribution for most aspect ratios.

10. The line-of-sight and single wall-reflected component for 1-MeV photons incident with isotropic fluence on a straight cylindrical duct in an Fe shield as a function of aspect ratio. The ratio of wall-reflection to line of sight component is at most about 10%.

10. Figures

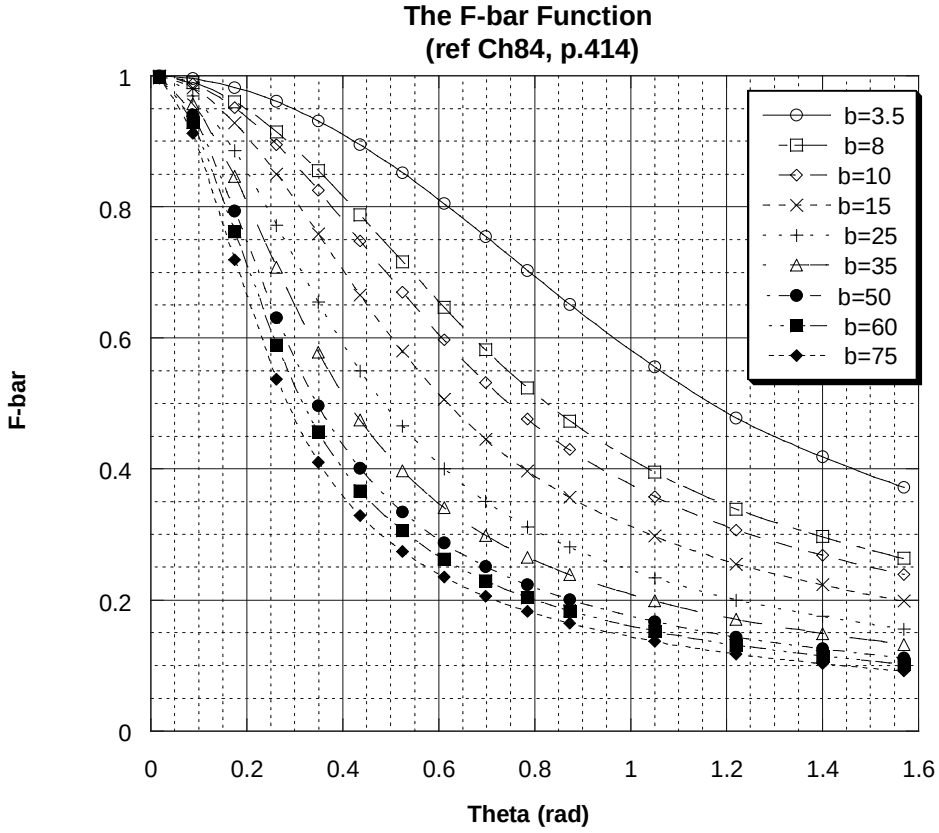

Figure 1

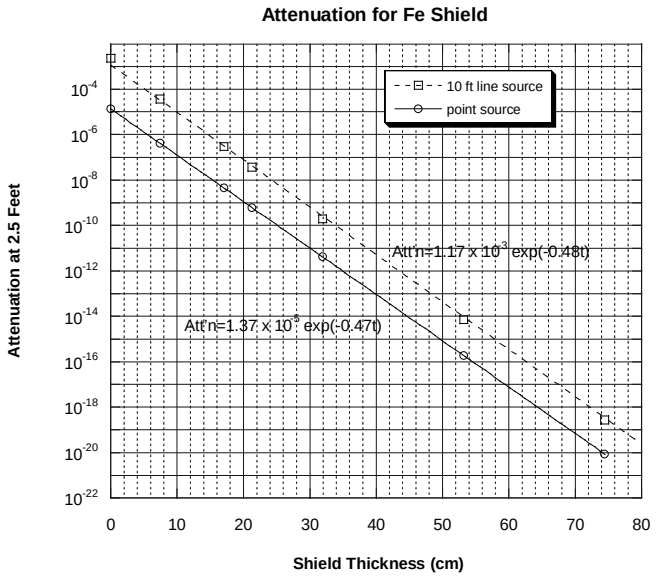
Attenuation for Fe Shield
Attenuation at 2.5 Feet
Shield Thickness (cm)
10 ft line source
point source
Att'n=1.17 x 10^3 exp(-0.48t)
Att'n=1.37 x 10^3 exp(-0.47t)

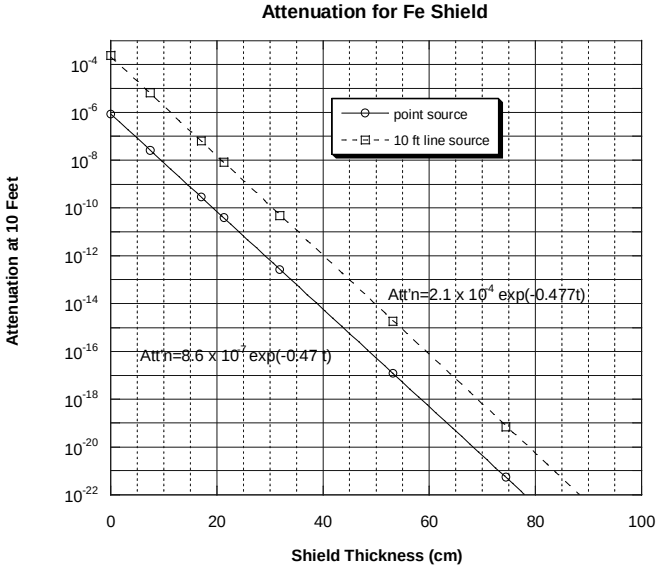
Attenuation for Fe Shield
Attenuation at 10 Feet
Shield Thickness (cm)
point source
10 ft line source
Att'n=2.1 x 10^4 exp(-0.477t)
Att'n=8.6 x 10^7 exp(-0.47 t)

Figure 2

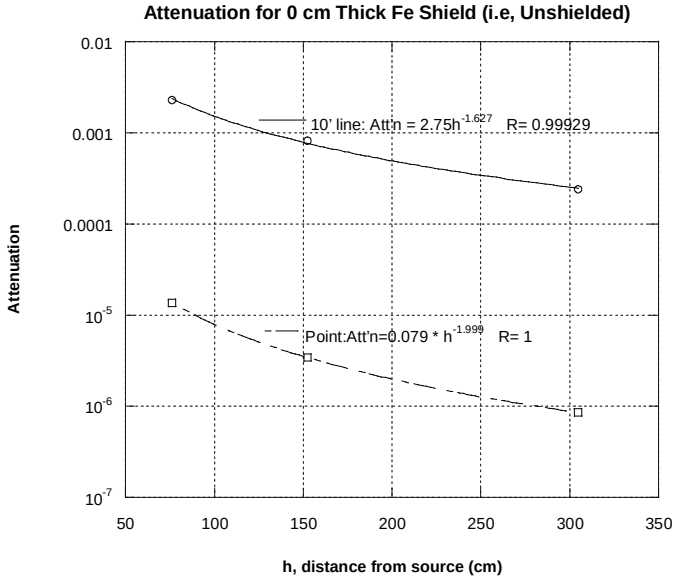
Attenuation for 0 cm Thick Fe Shield (i.e, Unshielded)
0.01
0.001
0.0001
10-5
10-6
10-7
Attenuation
10' line: Att'n = 2.75h-1.627 R= 0.99929
Point:Att'n=0.079 * h-1.999 R= 1
50
100
150
200
250
300
350
h, distance from source (cm)

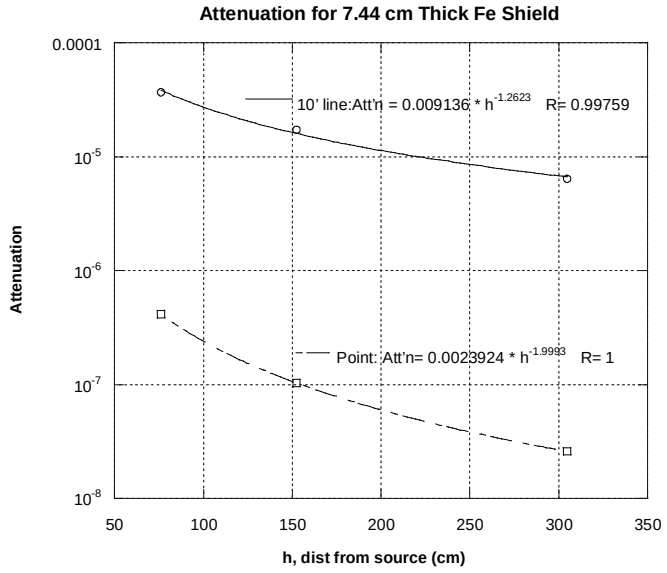
Attenuation for 7.44 cm Thick Fe Shield
0.0001
10-5
10-6
10-7
10-8
Attenuation
10' line:Att'n = 0.009136 * h-1.2623 R= 0.99759
Point: Att'n= 0.0023924 * h-1.9993 R= 1
50
100
150
200
250
300
350
h, dist from source (cm)

Figure 3

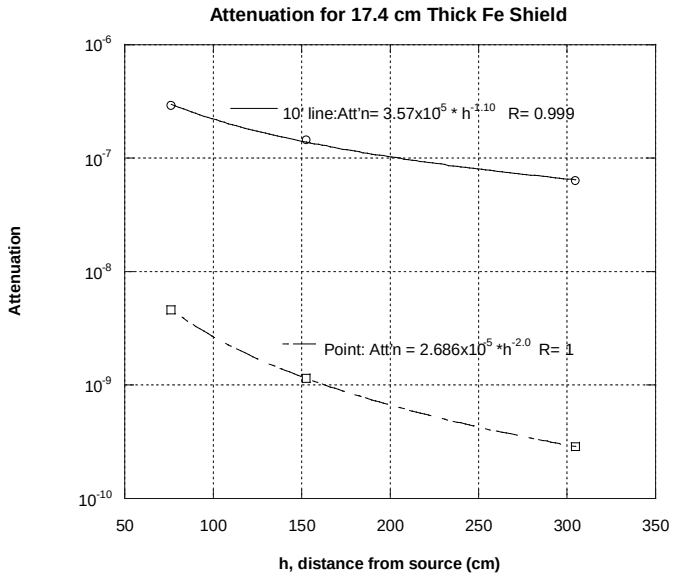
Attenuation for 17.4 cm Thick Fe Shield
10' line:Att'n= 3.57x10^5 * h^-1.10 R= 0.999
Point: Att'n = 2.686x10^5 *h^-2.0 R= 1
Attenuation
h, distance from source (cm)

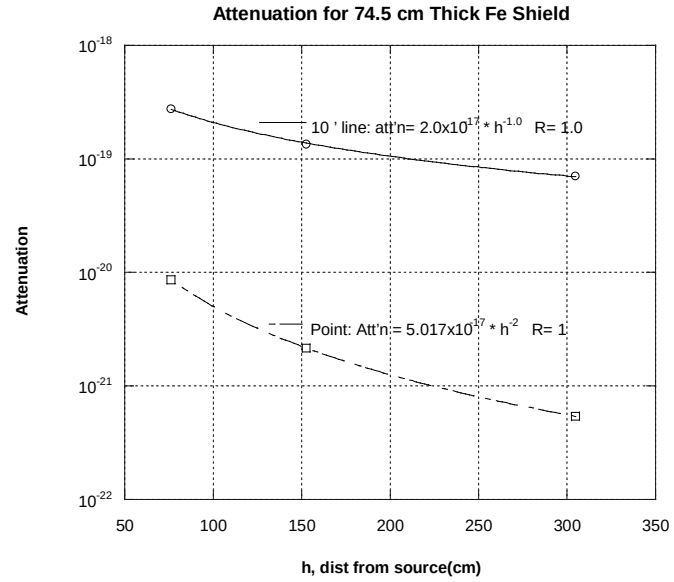
Attenuation for 74.5 cm Thick Fe Shield
10 ' line: att'n= 2.0x10^17 * h^-1.0 R= 1.0
Point: Att'n= 5.017x10^17 * h^-2 R= 1
Attenuation
h, dist from source(cm)

Figure 4

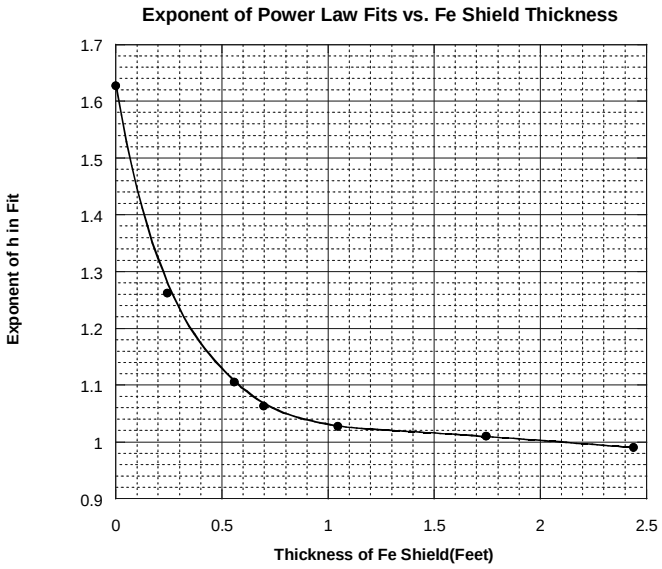
Exponent of Power Law Fits vs. Fe Shield Thickness
Exponent of h in Fit
1.7
1.6
1.5
1.4
1.3
1.2
1.1
1
0.9
0
0.5
1
1.5
2
2.5
Thickness of Fe Shield(Feet)

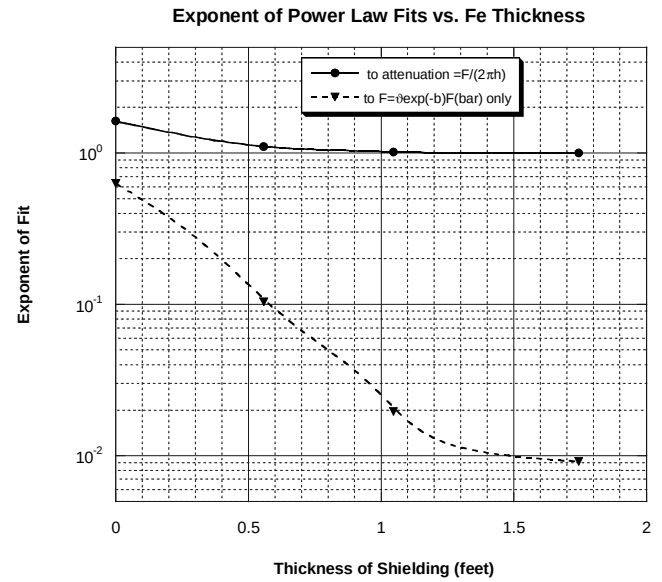
Exponent of Power Law Fits vs. Fe Thickness
to attenuation =F/(2πh)
to F=∂exp(-b)F(bar) only
Exponent of Fit
10^0
10^-1
10^-2
0
0.5
1
1.5
2
Thickness of Shielding (feet)

Figure 5

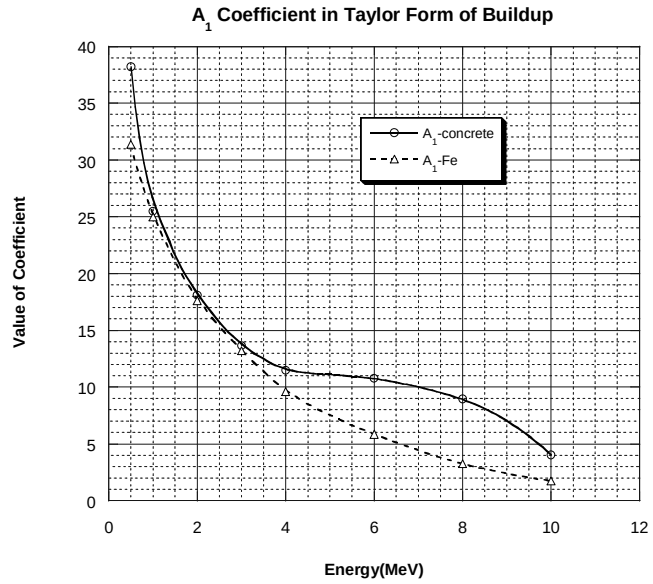
A1 Coefficient in Taylor Form of Buildup
Value of Coefficient
Energy(MeV)
A1-concrete
A1-Fe
0
5
10
15
20
25
30
35
40
0
2
4
6
8
10
12

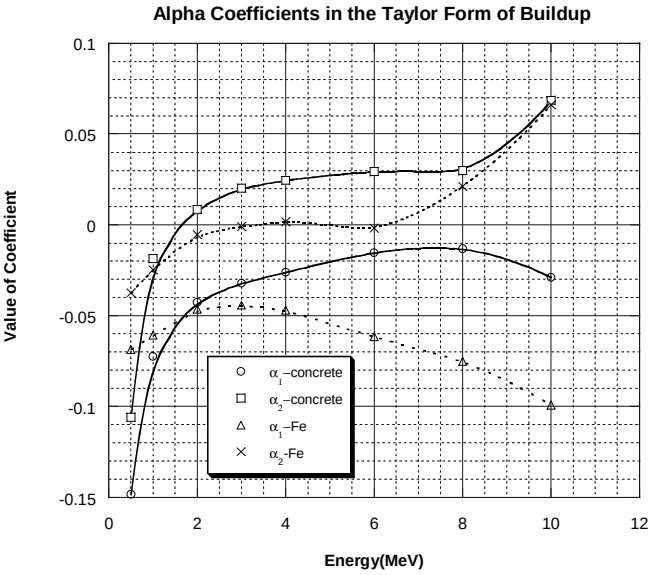
Alpha Coefficients in the Taylor Form of Buildup
Value of Coefficient
Energy(MeV)
α1–concrete
α2–concrete
α1–Fe
α2-Fe
0.1
0.05
0
-0.05
-0.1
-0.15
0
2
4
6
8
10
12

Figure 6

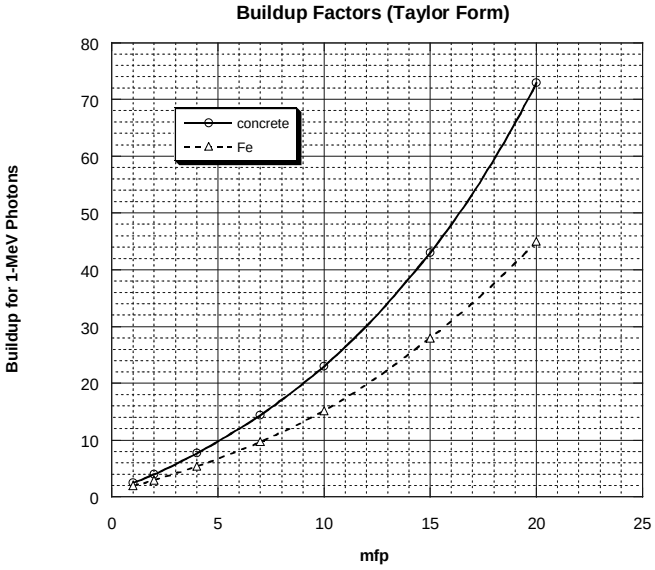
Buildup Factors (Taylor Form)
Buildup for 1-MeV Photons
mfp
concrete
Fe
0
10
20
30
40
50
60
70
80
0
5
10
15
20
25

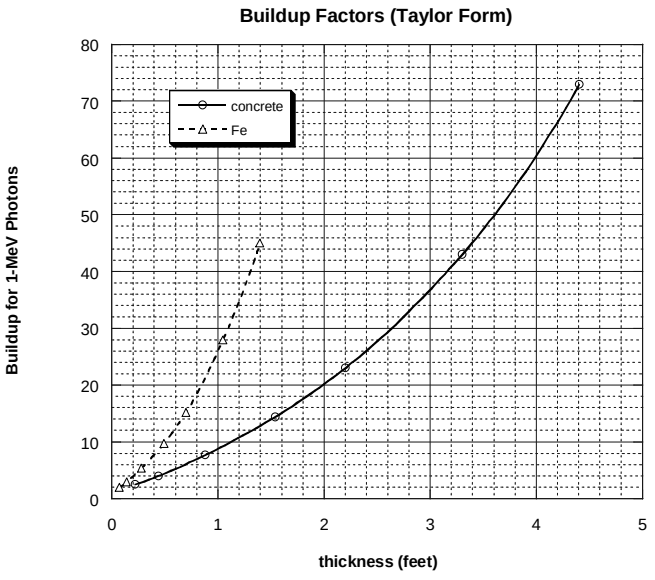
Buildup Factors (Taylor Form)
Buildup for 1-MeV Photons
thickness (feet)
concrete
Fe
0
10
20
30
40
50
60
70
80
0
1
2
3
4
5

Figure 7

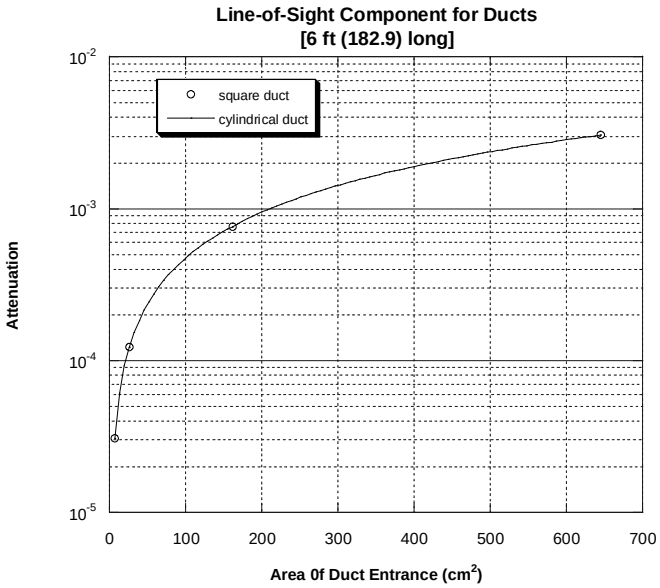
Line-of-Sight Component for Ducts
[6 ft (182.9) long]
square duct
cylindrical duct
Attenuation
10^{-2}
10^{-3}
10^{-4}
10^{-5}
0
100
200
300
400
500
600
700
Area 0f Duct Entrance (cm^2)

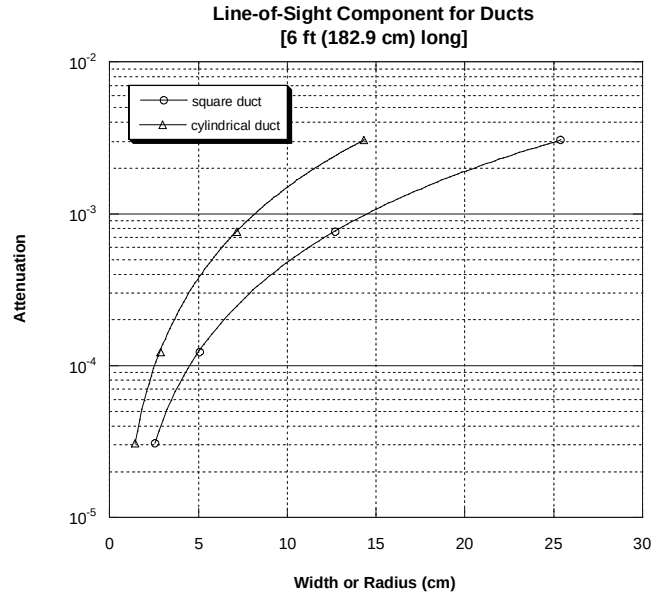
Line-of-Sight Component for Ducts
[6 ft (182.9 cm) long]
square duct
cylindrical duct
Attenuation
10^{-2}
10^{-3}
10^{-4}
10^{-5}
0
5
10
15
20
25
30
Width or Radius (cm)

Figure 8

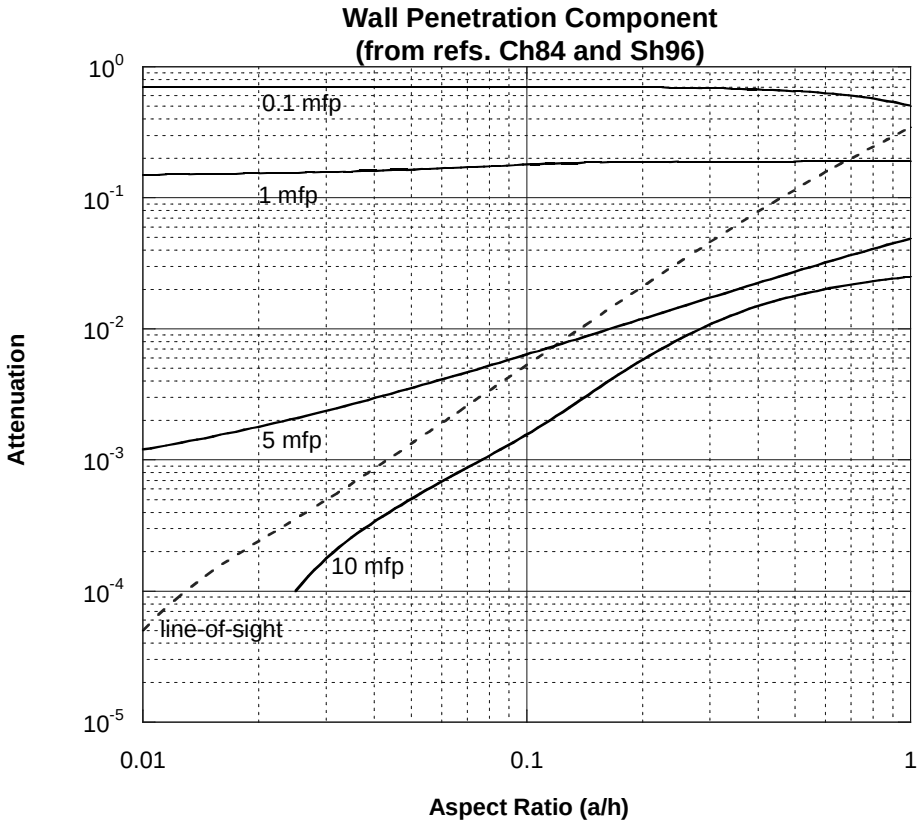
Wall Penetration Component
(from refs. Ch84 and Sh96)
Attenuation
10^{0}
10^{-1}
10^{-2}
10^{-3}
10^{-4}
10^{-5}
0.1 mfp
1 mfp
5 mfp
10 mfp
line-of-sight
0.01
0.1
1
Aspect Ratio (a/h)

Figure 9

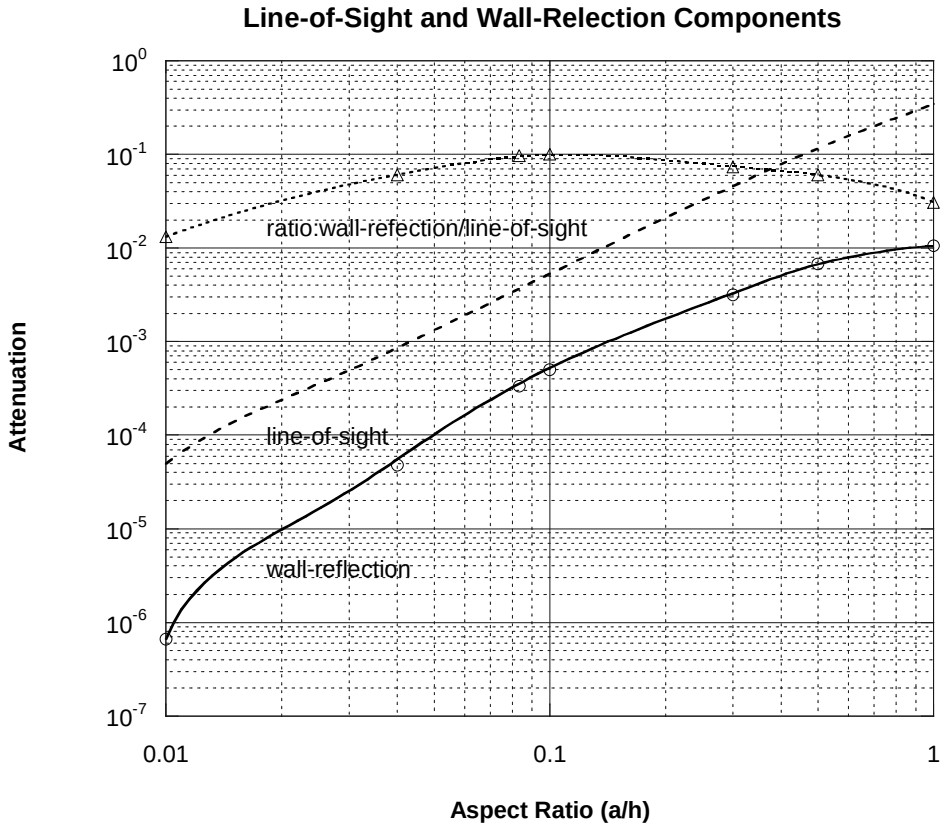
Line-of-Sight and Wall-Relection Components
Attenuation
10^{0}
10^{-1}
10^{-2}
10^{-3}
10^{-4}
10^{-5}
10^{-6}
10^{-7}
ratio:wall-refection/line-of-sight
line-of-sight
wall-reflection
0.01
0.1
1
Aspect Ratio (a/h)

Figure 10